

Compatibilization of blends of polystyrene and zinc salt of sulfonated polystyrene by poly(styrene-*b*-4-vinylpyridine) diblock copolymer

Shengqing Xu, Tao Tang, Bin Chen, Baotong Huang*

Changchun Institute of Applied Chemistry, Chinese Academy of Sciences, Changchun 130022, People's Republic of China

Received 1 December 1997; revised 13 May 1998; accepted 2 June 1998

Abstract

The compatibilizing effect and mechanism of poly(styrene-*b*-4-vinylpyridine) diblock copolymer, P(S-*b*-4VPy), on the immiscible blend of polystyrene (PS)/zinc salt of sulphonated polystyrene (Zn-SPS) were studied. SEM results show that the domains of the dispersed phase in the blend become finer. DSC experiments reveal that the difference between the two T_g 's corresponding to the phases in the blends becomes larger on addition of P(S-*b*-4VPy), mainly resulting from dissolving of the poly(4-vinylpyridine) (P4VPy) block in the Zn-SPS phase. FTIR analysis shows that compatibility of P4VPy and Zn-SPS arises from the stoichiometric coordination of the zinc ions of Zn-SPS and pyridine nitrogens of P4VPy. SAXS analysis indicates the effect of the P(S-*b*-4VPy) content on the structure of the compatibilized blends. When the content of the block copolymer is lower than 4.1 wt%, the number of ion pairs in an aggregate in the Zn-SPS becomes smaller, and aggregates in ionomer in the blend become less organized with increasing P(S-*b*-4VPy). When the P(S-*b*-4VPy) content in the blend is up to 7.4 wt%, a fraction of P(S-*b*-4VPy) form a separate domain in the blend. © 1999 Elsevier Science Ltd. All rights reserved.

Keywords: Polymer blends; Compatibilization; Block copolymer

1. Introduction

The blending of polymers has been the subject of intense research activities in both academic and industrial laboratories. The motivations in the enormous interest in polymer blends are the lower cost in developing a new polymer and the shorter period between development and commercial production [1,2].

In general, polymer blends of two or more components exhibit poor mechanical properties due to immiscibility resulting from lower entropy of mixing of high molecular weight polymers and the unfavorable enthalpic interaction between the components [1,2]. One means to improve the miscibility of polymers is to provide specific interaction sites on the polymer chains providing a negative heat of mixing [2]. Another means of enhancement in the degree of compatibility between the components is to add a compatibilizer. A block or a graft copolymer has been known to be effective in reducing interfacial tension and improving the interfacial adhesion between the blend components through entanglements or bridging chains of different polymers near the interface [3–5].

Polystyrene (PS) is a commodity polymer with high

brittleness. One of the most useful methods to increase its toughness is to add rubbery particles or rigid particles as a second phase. The former has been successfully used in toughening PS, as in high-impact polystyrene (HIPS), acrylonitrile–butadiene–styrene copolymer (ABS) and styrene–butadiene–styrene triblock copolymer (SBS). The latter has been widely used, and the rigid particles used are often rigid-particular fillers, such as glass beads and silica. In contrast to these rigid fillers, a polymer whose T_g is above room temperature may be used as a more effective second phase [6–8]. There are several factors to influence the fracture behavior of the two-component system [6–8], such as the type of the polymer as the second phase, the blend composition, the preparation conditions and the compatibility of the blend.

Ionic polymers, or ionomers, containing a small amount of pendent ionic groups chemically bound to a non-polar chain, have dramatic effects on the properties of polymers, leading to a range of specific industrial applications [9–11]. Such ionomers develop strong intermolecular interactions due to the presence of the ionic moieties, and they possess a unique microstructure. Most ionomers consist of two phases, one a matrix phase containing dispersed ionic multiplets, i.e. nano-size aggregates of interacting ion pairs, and the other an ion-rich, more chain-entangled cluster 'phase'

* Corresponding author.

that consists of regions of restricted chain mobility surrounding multiplets [12]. Although most ionomers are typically not miscible with their parent non-polar polymers [13,14], introduction of such ionic groups substantially increases the miscibility of the non-polar polymer with other polar polymers. Therefore, ionomers and their interactions in blends with other polymers have been widely studied [15–20].

Metal alkali salts of lightly sulphonated polystyrene (SPS) generally have much higher melt viscosities and solution viscosities than the analogous unfunctionalized polystyrene [9]. In the present work, Zn^{2+} was chosen over alkali metals primarily because it consistently produces a lower ionomer melt viscosity than other metal counterions [9,21]. In addition, the zinc salt (Zn-SPS) can be easily obtained, and it has good mechanical properties even at elevated temperatures, i.e. above T_g . According to the above theory about toughening PS, Zn-SPS is expected to be an appropriate polymer to toughen PS. Regrettably, the miscibility of PS and Zn-SPS (sulphonation 7.82 mol%) is too poor; thus, it is necessary to improve their miscibility.

In the present study, poly(styrene-*b*-4-vinylpyridine) diblock copolymer, P(S-*b*-4VPy), is tested as a compatibilizer of PS/Zn-SPS blend. Besides the miscibility between the one block polystyrene (PS) and the PS homopolymer, the poly(4-vinylpyridine) (P4VPy) block, as a Lewis polybase, is widely miscible with several acidic polymers such as polyacids [22,23], poly(hydroxy ether of bisphenol A) [24] and poly(vinyl phenol) [25] due to specific interactions. Anionic synthesis of the diblock copolymer makes its architecture and composition easily controllable. In this work, the blend composition of PS/Zn-SPS is chosen as 70/30 (wt/wt), which is based on the consideration that the ionomer at this level has an effective toughening effect on PS [13]. The compatibilizing effect of P(S-*b*-4VPy) on PS/Zn-SPS blends, the compatibilization mechanism of P(S-*b*-4VPy) and the structure of the compatibilized blends were investigated.

2. Experimental

2.1. Materials

The blend component polystyrene, PS, synthesized via anionic polymerization, has a number-average molecular weight (M_n) and polydispersity index (M_w/M_n) of 3.09×10^4 and 1.06, respectively, as determined by Gel-Permeation Chromatography (g.p.c.) using calibration curves for standard polystyrene.

The free-radically polymerized polystyrene with $M_n = 1.61 \times 10^5$ and $M_w/M_n = 1.93$ purchased from Yanshan Petrochem. Co. was chosen as the starting material for preparation of the zinc salt of sulphonated polystyrene (Zn-SPS). The Zn-SPS was prepared via the following two-step procedure documented in the literature [26,27]. The

commercial PS was dissolved in toluene and precipitated in methanol to remove residuals. After air and vacuum drying, the polymer was dissolved in chloroform, and sulphonated with acetyl sulphonate generated from sulphuric acid and acetic anhydride. The sulphonated polystyrene (SPS) was isolated by pouring the reaction mixture into boiling water, then it was extracted with water until the extract titrated neutral. Samples were vacuum-dried and analysed for sulphur content to determine the sulphonation level via elementary analysis. The degree of sulphonation of Zn-SPS was 7.82 mol%. The obtained SPS was dissolved in tetrahydrofuran (THF), and 50% excess of the stoichiometric amount of aqueous $\text{Zn}(\text{CH}_3\text{COO})_2$ was added and kept at 50°C for more than 5 hours in order that the acid groups were completely neutralized (tracing the zinc content with atomic absorption spectrometry). The polymer solution was precipitated into a mixture of water and methanol, and the precipitate was collected, dried in air and then in vacuo.

Poly(styrene-*b*-4-vinylpyridine), P(S-*b*-4VPy), was synthesized via sequential anionic copolymerization [28,29]. The product was extracted successively with boiling cyclohexane and a mixture of ethanol/water (90/10). The final copolymer was characterized using g.p.c. and $^1\text{H-NMR}$. Its M_n and M_w/M_n were 7.32×10^4 and 1.10, respectively, and the content of PS block in it was 47 wt%.

Poly(4-vinylpyridine) (P4VPy) was prepared by anionic polymerization in THF at -78°C using *n*-BuLi/1,1-diphenyl ethylene as the initiator. Its M_n and M_w/M_n were 3.84×10^4 and 1.07, respectively.

2.2. Preparation of blends

All polymer materials were dried at 90°C in vacuo overnight before blending. The binary Zn-SPS/P4VPy blend system with three different blend compositions of 96.6/3.4, 93.2/6.8 and 88.4/11.6 (wt/wt), and the ternary PS/Zn-SPS blend system with different contents of P(S-*b*-4VPy) (0–7.4 wt%) based on the total amount of PS and Zn-SPS were prepared by a solution/precipitation method. For each blend, all polymer components were dissolved in chloroform, and then the mixture was agitated at room temperature until a homogeneous solution was formed. The solution was poured into a large amount of hexane, and the precipitate was dried under vacuum at 90°C for two days.

Blend samples were prepared by pressing in the mold in a hot press for 10 min at 170°C and 10 MPa, and then cooling to ambient temperature in air. The thickness of the sample for small-angle X-ray scattering (SAXS) measurement was 1.5 mm.

2.3. Testing and characterization

The fractured surface of a PS/Zn-SPS blend without or with P(S-*b*-4VPy) for scanning electron microscopy (SEM, JEOL JAX-84) observation was prepared by dipping the

sample in liquid nitrogen and then fracturing. The fractured surface was then etched with THF at room temperature to remove the PS phase. The morphology of the cryogenically fractured surface was observed after coating with gold.

Thermal analysis of the neat blend components as well as the blends was carried out using a Perkin-Elmer DSC-7 System under a nitrogen atmosphere. The heating rate was 30°C/min.

SAXS measurements were performed with an Anton-Paar Kratky Compact SAXS System.

Absolute intensities were obtained with a polyethylene strip traceable to a Lupolen standard [30]. The SAXS profile was corrected for background scattering [31] and the corrected profile was desmeared by the iterative method of Lake [32]. The data were presented on a consistent relative intensity scale, normalized for sample thickness and transmittance, as slit-desmeared intensity I_{des} (arbitrary unit) versus the scattering vector $q = (4\pi/\lambda)\sin\theta$, where λ is the radiation wavelength (0.154 nm) and 2θ the scattering angle.

Infrared spectra were obtained on a BIO RAD FTS-7 Fourier transform infrared (FTIR) spectrometer. The film specimen was obtained by casting on a NaCl plate from a 1.0 wt% solution of Zn-SPS/P4VPy blend in chloroform and then dried under vacuum.

3. Results and discussion

3.1. Compatibilizing effect of the block copolymer

3.1.1. Morphology

SEM micrographs of the etched, cryogenically fractured surfaces for the PS/Zn-SPS 70/30 (wt/wt) blends with different contents of P(S-*b*-4VPy) are presented in Fig. 1. The uncompatibilized blend of PS/Zn-SPS shows characteristics of an immiscible blend (Fig. 1a). The domains of the dispersed phase (Zn-SPS) are coarse and irregular. When 2.0 wt% of the block copolymer is added, the domain size of the dispersed phase becomes small (Fig. 1b). When the P(S-*b*-4VPy) amount is up to 4.1 wt%, which corresponds to the stoichiometric ratio of Zn²⁺ ions in Zn-SPS to pyridine nitrogens in P4VPy block, the domains of the dispersed phase in the blends become smaller (Fig. 1c). However, when the content of P(S-*b*-4VPy) is up to 7.3 wt%, the domain size of the dispersed phase does not change much (Fig. 1d). The SEM results indicate that the block copolymer acts as an effective compatibilizer.

3.1.2. Thermal analysis

The DSC thermograms of the specimens of the PS/Zn-SPS blends with different contents of P(S-*b*-4VPy) are shown in Fig. 2. The neat PS possesses a glass transition at 100.2°C and the transition region (ΔT_g) is 7.1°C (Fig. 2a). As a consequence of ionic aggregates in the neat Zn-SPS, it possesses a higher T_g and a larger ΔT_g , 122.2°C and 10.2°C,

respectively (Fig. 2b). It is apparent that the two glass transitions of PS and Zn-SPS do not overlap each other. For the neat P(S-*b*-4VPy), it possesses two T_g 's resulting from its microphase-separated structure, 104.7°C corresponding to the PS block, and 141.7°C to the P4VPy block.

On the DSC thermogram of the binary PS/Zn-SPS 70/30 (wt/wt) blend, two distinct T_g 's appear, indicating that the blend is immiscible: one is PS-rich phase and the other Zn-SPS-rich phase. When P(S-*b*-4VPy) with less than 4.1 wt% is added, the ternary blend still possesses two T_g 's. As the content of P(S-*b*-4VPy) increases, the lower T_g corresponding to the PS-rich phase keeps almost unchanged, and the upper T_g corresponding to the Zn-SPS-rich phase shifts slightly to a higher temperature. This can be interpreted in terms of the compatibilizing model using a block copolymer as compatibilizer [1]. Since the P4VPy block in P(S-*b*-4VPy) has a higher T_g than Zn-SPS, blending of the two polymers leads to a higher T_g of Zn-SPS if the P4VPy block can be dissolved in the Zn-SPS domain [33], as will be further proved in the next section of this paper.

When the content of P(S-*b*-4VPy) is up to 7.3 wt% (Fig. 2f), three T_g 's occur on the DSC curve of the compatibilized blend. The lowest transition corresponding to the PS-rich phase becomes broader; and the middle T_g corresponding to the Zn-SPS-rich phase is in accordance with the upper T_g of the compatibilized blend with 4.1 wt% of P(S-*b*-4VPy). The third T_g occurs at 141.3°C, which is just the same as the T_g of the P4VPy block of P(S-*b*-4VPy). The appearance of the third T_g , though its transition is weak, may imply that the content of P(S-*b*-4VPy) (7.3 wt%) in the PS/Zn-SPS blend is higher than its saturated concentration at the interface, and part of P(S-*b*-4VPy) forms a separated phase in the blend, probably in the form of micelles [34,35]. From the DSC results it is believed that P(S-*b*-4VPy) with a small content in the PS/Zn-SPS blend can play a role as a compatibilizer.

3.1.3. Miscibility and structure of P(S-*b*-4VPy) blends

The molecular weight of PS block in P(S-*b*-4VPy) being higher than that of the PS homopolymer in the PS/Zn-SPS blend partly meets the demand of a block copolymer to be a compatibilizer [29,34]. However, full or partial miscibility of Zn-SPS and the P4VPy block is necessary for the block copolymer to act as an effective compatibilizer. A model polymer, P4VPy homopolymer, with the same molecular parameters as the P4VPy block in P(S-*b*-4VPy), instead of the P4VPy block, was used to estimate the compatibility of P4VPy and Zn-SPS, the nature of the special interaction between the two polymers, and the microstructure of the Zn-SPS/P4VPy blends.

3.1.4. Compatibility of Zn-SPS and P4VPy

Fig. 3 shows DSC thermograms of homo-P4VPy and the Zn-SPS/P4VPy blends of different blend compositions. The T_g 's are listed in Table 1. When the content of P4VPy in the blend is lower than 6.8 wt%, i.e. Zn-SPS/

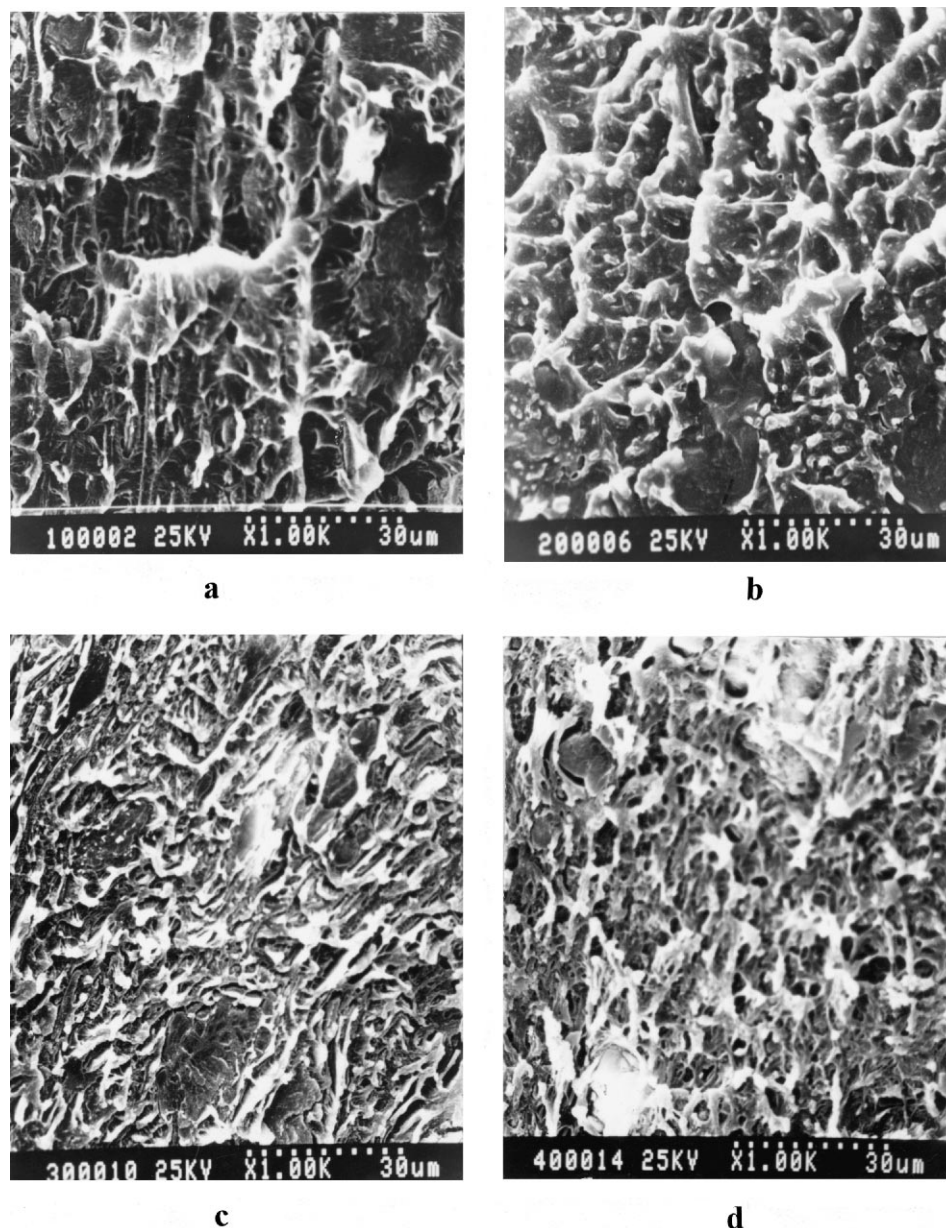


Fig. 1. Morphologies of etched, fractured surfaces for PS/Zn-SPS 70/30 (wt/wt) blends with different contents (wt% based on total PS and Zn-SPS, i.e. amount of P(S-*b*-4VPy) divided by the total amount of PS and Zn-SPS): (a) 0, (b) 2.0, (c) 4.1, and (d) 7.3. The black domains in all micrographs correspond to the PS phase.

P4VPy 93.2/6.8 (wt/wt), which is the stoichiometric ratio of zinc ions in Zn-SPS to pyridine nitrogens of P4VPy, Zn-SPS/P4VPy blend possesses only one single glass transition, indicating the two polymers are miscible in the range of blend composition. The corresponding T_g of the blends shows positive deviation from T_g values calculated by Fox's equation [36]. Usually, for blends with strong specific interactions between the components, blending leads to similar results [24,25].

When the content of P4VPy in the blend is up to 11.6 wt%, two T_g 's appear, the lower one being the T_g of the Zn-SPS/P4VPy 93.2/6.8 (wt/wt) blend, and the upper

one being close to that of P4VPy. Thus, miscibility is not achieved, and the blend has a two-phase structure: a mixed Zn-SPS/PS phase and a P4VPy-rich phase. On the other hand, the insensitivity of the high-temperature transition to blending indicates that the composition profiles across the interface between the two phases in the blend may be asymmetric [37].

3.1.5. Nature of the interaction between Zn-SPS and P4VPy

The representative infrared spectra of neat Zn-SPS, neat P4VPy and the Zn-SPS/P4VPy 93.2/6.8 (wt/wt) blend are shown in Fig. 4. The absorptions of the infrared spectrum of

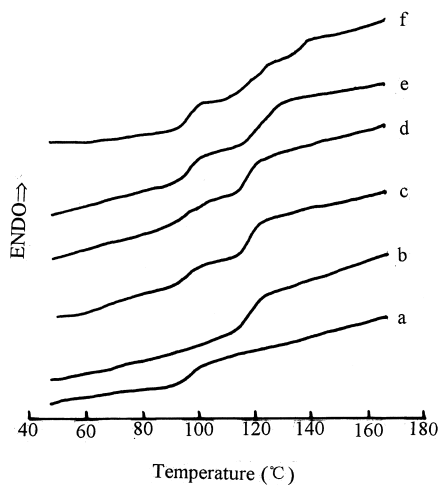


Fig. 2. DSC thermograms of neat PS (a), neat Zn-SPS (b), and PS/Zn-SPS 70/30 blends with: (c) 0, (d) 2.0 wt%, (e) 4.1 wt%, and (f) 7.3 wt% P(S-*b*-4VPy).

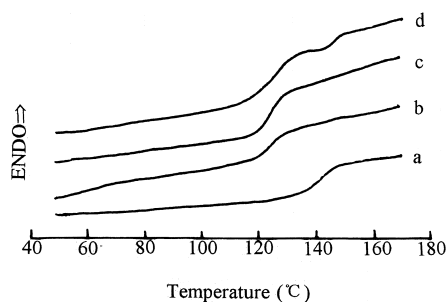


Fig. 3. DSC thermograms of Zn-SPS/P4VPy blends of different composition (wt/wt): (a) 0/100, (b) 96.6/3.4, (c) 93.2/6.8, and (d) 88.4/11.6.

neat Zn-SPS in the region of 800–1800 cm^{-1} have been assigned by Fitzgerald and Weiss [38,39]. The sharp peak at 1002 cm^{-1} is assigned to the in-plane vibration of the para-substituted benzene ring, the peak centred at 1042 cm^{-1} and the broad band at 1100–1200 cm^{-1} are ascribed to the symmetric stretching of O=S=O, a sharp peak at 1270 cm^{-1} is attributed to the asymmetric stretching mode of O=S=O. Since no characteristic band of the stretching of –OH groups in the range of 3000–3600 cm^{-1} is

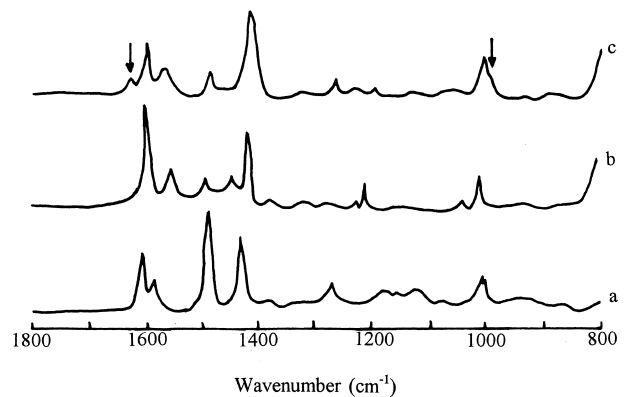


Fig. 4. IR spectra of Zn-SPS (a), P4VPy (b) and Zn-SPS/P4VPy 93.2/6.8 (wt/wt) blend (c).

observed for Zn-SPS dried for a long time at 90°C in vacuo, the ionomer has no water in the ionic clusters [38]. On the infrared spectrum of P4VPy, the peaks at 1413, 1554 and 1595 cm^{-1} are all related to the rocking vibration of the ring-substituted pyridine groups [39].

On the infrared spectrum of the Zn-SPS/P4VPy blend, the appearance of an absorption at 1621 cm^{-1} (arrow at left in Fig. 4c) in the blend can be assigned to the stretching vibration mode of the pyridinium cation [39]. In addition, blending of Zn-SPS and P4VPy causes a new peak to appear at 980 cm^{-1} (arrow at right in Fig. 4c) and the peak at 1002 cm^{-1} to decrease compared to the spectrum of Zn-SPS. Since the peak at 1002 cm^{-1} is a substituent-sensitive band of in-plane vibration for the benzene ring [38], the peak at 980 cm^{-1} is considered to result from a shift of the peak at 1002 cm^{-1} due to the interaction between Zn-SPS and P4VPy. The interaction by coordination between zinc ions in Zn-SPS and pyridine nitrogens of P4VPy is by a stoichiometric ratio [40,41].

3.1.6. Structure of the Zn-SPS/P4VPy blends

The influence of the added P4VPy on the microstructure of Zn-SPS was investigated by SAXS analysis of Zn-SPS/P4VPy blends of different compositions (Fig. 5). The only peak in the pattern of the neat Zn-SPS near $q = 1.7 \text{ nm}^{-1}$ is typical for metal-neutralized sulphonated ionomers [42,43]

Table 1
Data of T_g 's of Zn-SPS/P4VPy blends of different compositions

Composition of Zn-SPS/P4VPy (wt/wt)	The corresponding content of P(S- <i>b</i> -4VPy) in the compatibilized blends (wt%)	$T_g/^\circ\text{C}$	
		$T_{g\text{obs}}/^\circ\text{C}^{\text{a}}$	$T_{g\text{cal}}/^\circ\text{C}^{\text{b}}$
100/0	–	122.2	–
96.6/3.4	2.0	123.7	122.6
93.2/6.8	4.1	124.6	123.8
88.4/11.6	7.3	124.6; 141.4	–
0/100	–	142.1	–

^aMeasured by DSC.

^bEstimated by Fox's equation [36].

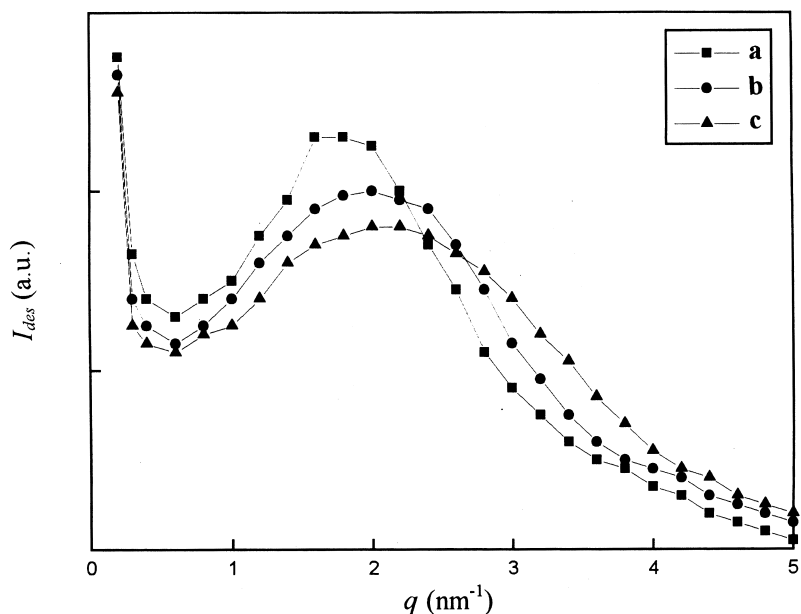


Fig. 5. SAXS patterns of Zn-SPS/P4VPy blends of different composition (wt/wt): (a) 100/0, (b) 96.6/3.4, and (c) 93.2/6.8.

and is evidence for the presence of ionic aggregates in the material. Morphological models proposed for the microstructure of such random ionomers typically treat the SAXS maximum (termed the ‘ionic peak’) as arising from either interparticle [42,44] or intraparticle [45,46] interferences. Nevertheless, the fact that ionomer morphology can be modeled from two completely different interpretations of the experimental data, and the fact that many assumption or adjustable parameters are needed to fit models to the SAXS data, suggest that much work remains to be done in this area. Here, we try to analyse the experimental data only using the interparticle scattering models which suggest that a fraction of ion pairs in random ionomers exist as lone ion pairs in the matrix.

The application of Bragg’s law to the first peak gives a characteristic distance, d_{Bragg} , which is directly proportional to the average centre-to-centre distance, d , between ionic aggregates, and d_{Bragg} is obtained from the peak maximum ($d_{\text{Bragg}} = 2\pi/q^*$, where q^* is the scattering vector of the first peak, named the ‘peak position’). The d_{Bragg} is related to the average number of ion pairs per aggregate, n_i , and the extent of these ion pairs’ orderly-packing in an aggregate [47]. The

n_i value is estimated by the following equations [48]

$$n_i = \rho N(d_{\text{Bragg}})^3 / EW \quad (1)$$

or

$$n_i \propto (d_{\text{Bragg}})^3 \quad (2)$$

where ρ is the ionomer density, N Avogadro’s number, and EW the ionomer equivalent weight.

Only one ionic peak in the q -range of 1.5–2.5 nm^{-1} is observed in the SAXS patterns (Fig. 5) of Zn-SPS/P4VPy blends with different compositions, shifting to a higher q and becoming broader with P4VPy. Table 2 summarizes the Bragg distance (d_{Bragg}) estimated by Eq. (2), the relative value of the number of ion pairs per aggregate, n_i/n_0 (n_0 , n_i are the number of ion pairs per aggregate in neat Zn-SPS and in Zn-SPS blend, respectively), and the quantitative measure of the SAXS peak width, $\Delta q_{2/3}/q^*$ (where $\Delta q_{2/3}$ is the width in scattering vector at $q = 2/3 q^*$ on the SAXS profile, and q^* is the peak (position) of the Zn-SPS/P4VPy blends. These data show that all of the morphological parameters of the blends obtained from the SAXS profiles are distinctly influenced by the P4VPy content. Inspection

Table 2
SAXS data of Zn-SPS and Zn-SPS/P4VPy blends

Composition of Zn-SPS/P4VPy (wt/wt)	q^*/nm^{-1}	$d_{\text{Bragg}}/\text{nm}^{-1}$	n_i/n_0^a	$\Delta q_{2/3}/q^{*b}$
100/0	1.7	3.7	1	0.75
96.6/3.4	1.9	3.3	0.71	0.95
93.2/6.8	2.1	3.0	0.53	1.10

^a n_0 , number of ion pairs per aggregate in neat Zn-SPS; n_i/n_0 from Eq. (2).

^bPeak width at $q = 2/3 q^*$ divided by this peak position (q^*).

of the d_{Bragg} and $\Delta q_{2/3}/q^*$ data within the two Zn-SPS/P4VPy blends shows that the ionic peak shifts to a lower d_{Bragg} (i.e. higher q^*) and becomes broader (i.e. larger $\Delta q_{2/3}/q^*$) with P4VPy. Meanwhile, there is a decrease in the number of ion pairs per aggregate (n_i) as the content of P4VPy increases. All the results arise from the compatibility of Zn-SPS and P4VPy, as can be interpreted as follows: upon blending of Zn-SPS and P4VPy, the coordination of the zinc ions in Zn-SPS and the pyridine nitrogens in P4VPy leads to disintegration of a part of the ion pairs in the aggregate, i.e. decrease in n_i . In the case of sulphonated polystyrene ionomers, rheological measurements [16] have shown that trialkyl ammonium counterions effectively suppress ionic interactions due to steric hindrance. Coordination to an entire polymer chain through pyridine groups should have a similar effect, causing a broader distribution in the aggregate size, i.e. a larger $\Delta q_{2/3}/q^*$; thus, the aggregates in the ionomer in the blend become less organized.

3.2. Structure of the compatibilized blends

Fig. 6 shows a comparison of the SAXS patterns for the PS/Zn-SPS blends with different P(S-*b*-4VPy) contents. The peak in the pattern of neat P(S-*b*-4VPy) near $q = 0.3 \text{ nm}^{-1}$ indicates that the block copolymer has a typical microphase-separated structure and that it has a larger microdomain size than Zn-SPS [34].

The peak position and width of the binary PS/Zn-SPS 70/30 (wt/wt) blend are virtually identical with those of the neat Zn-SPS, implying that the morphology of ionic aggregates in Zn-SPS in the blend is very similar to that in the neat Zn-SPS (Fig. 5a), the added PS having no notable effect on the structure of the ionomer. Therefore, the changes in the SAXS peak of the ternary PS/Zn-SPS/P(S-*b*-4VPy) are

mainly caused by the addition of P(S-*b*-4VPy), i.e. the block copolymer has an effect on the morphology of Zn-SPS, which can be proved by the SAXS experiment. The aggregates in Zn-SPS are maintained even on addition of 2.0 wt% and 4.1 wt% of P(S-*b*-4VPy) in the PS/Zn-SPS blend (Fig. 6c,d); however, an increase in the content of the block copolymer leads to a broader ionic peak at a higher scattering vector.

Firstly, let us discuss the effect of the P(S-*b*-4VPy) content on the SAXS peak width. If the ionic peaks are attributed to a collection of scatterings from particles arranged in a paracrystalline lattice, the peak maximum then represents an estimate of the average repeat distance [49]. From this argument, the $\Delta q_{2/3}/q^*$ results suggest that the ionomer in the compatibilized blend with lower P(S-*b*-4VPy) content contains ionic aggregates with a narrower distribution of scattering distances, and the ionomer is better organized due to smaller steric hindrance between the ionic groups and easier motion of polymer chains.

Next, we see that the general morphological characteristics of the ionomers in blends are influenced by the P(S-*b*-4VPy) content. The ionic peak shifts to a lower q , i.e. d_{Bragg} increases with P(S-*b*-4VPy) (Fig. 6). This consideration involves the relative ability of the ion pairs to pack into organized ionic aggregates. When the ion pairs aggregate, the bounded polymer chains of the Zn-SPS resulting from the coordination between Zn-SPS and the P4VPy block of P(S-*b*-4VPy) encountered during order-packing limited the number of ion pairs incorporated into the aggregate [50]; in other words, because the polymer chains move with more difficulty, a smaller number of the ion pairs enter the aggregates, and thus d_{Bragg} increases.

For blends with different contents of P(S-*b*-4VPy), the P(S-*b*-4VPy) content was observed to influence the overall

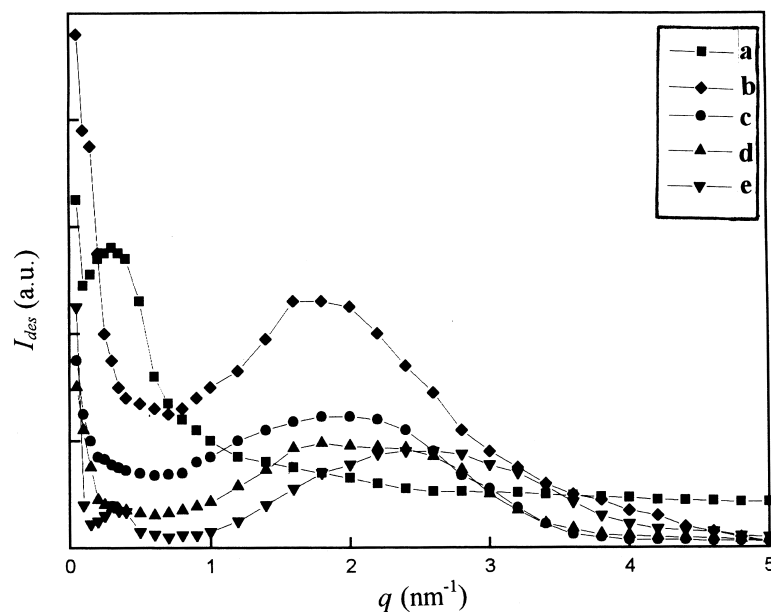


Fig. 6. SAXS patterns of neat P(S-*b*-4VPy) (a) and PS/Zn-SPS 70/30 (wt/wt) blends with: (b) 0, (c) 2.0 wt%, (d) 4.1 wt%, and (e) 7.3 wt% P(S-*b*-4VPy).

organization of the ion pairs in aggregate. The ion pairs become less organized with increasing P(S-*b*-4VPy), resulting in a broader SAXS peak at a higher q value. Related to the SAXS results of the Zn-SPS/P4VPy blends, it can be seen that there are the P4VPy blocks in P(S-*b*-4VPy) dissolving into the Zn-SPS domains in the ternary blend.

Above all, considering the immiscibility of P(S-*b*-4VPy) and the two blend components, PS and Zn-SPS, and the compatibilizing effect of the block copolymers, it may be suggested that a small amount of P(S-*b*-4VPy) tends to be situated at the interface between the PS and the Zn-SPS phases and the blocks penetrate into their corresponding phases [51–53], i.e. the PS block into the PS phase and the P4VPy block into the Zn-SPS phase.

At a P(S-*b*-4VPy) content of 7.4 wt%, a new weak peak appears near $q = 0.3 \text{ nm}^{-1}$, corresponding to the peak position of the neat P(S-*b*-4VPy) (Fig. 6a), implying that part of P(S-*b*-4VPy) forms a separate phase, probably micelles [34,35]. Thus, 7.4 wt% is higher than the micelle concentration (CMC) of P(S-*b*-4VPy) in the PS/Zn-SPS blend, which is higher than 4.1 wt%, the stoichiometric ratio of zinc ions in Zn-SPS to pyridine nitrogens in P(S-*b*-4VPy).

4. Conclusions

Diblock copolymer poly(styrene-*b*-4-vinylpyridine), P(S-*b*-4VPy), synthesized by anionic copolymerization, acts as an effective compatibilizer for immiscible blend of PS/Zn-SPS. The compatibilizing effect and mechanism of P(S-*b*-4VPy) were studied by various techniques. SEM shows finer domains of the dispersed phase. The difference between the two T_g 's corresponding to the two phases becomes larger on addition of P(S-*b*-4VPy), as P4VPy block was dissolved into the Zn-SPS phase. FTIR analysis indicates compatibility between Zn-SPS and P4VPy arising from specific interaction between them through stoichiometric coordination of zinc ions of Zn-SPS and pyridine nitrogens.

The effect of P(S-*b*-4VPy) content on the structure of the compatibilized blends was further investigated. When the P(S-*b*-4VPy) content is lower than 4.1 wt%, the ion pairs in aggregates in Zn-SPS in the compatibilized blends become less organized, and the number of ion pairs per aggregate becomes smaller with increasing P(S-*b*-4VPy), resulting in broader SAXS peaks at higher q values. When the P(S-*b*-4VPy) content is up to 7.4 wt%, a new peak occurring at the same position as that of neat P(S-*b*-4VPy) corresponds to a separate domain of the diblock copolymer in the blend.

Acknowledgements

This work was part supported by the National Natural Science Foundation of China (Grant no. 59503002) and the Polymer Physics Laboratory of Changchun Institute of Applied Chemistry, Chinese Academy of Sciences.

References

- [1] Paul DR, Newman S. Polymer blends, vol. 2. New York: Academic Press, 1978.
- [2] Folkes MJ, Hope PS. Polymer blends and alloys. London: Blackwells, 1993.
- [3] Brown HR. *Macromolecules* 1989;22:2859.
- [4] Fayt R, Jerome R, Teyssie Ph. *J Polym Sci Polym Phys Ed* 1989;27:775.
- [5] Creton C, Kramer EJ, Hadziioannou G. *Macromolecules* 1991;24:1846.
- [6] Trent JS, Scheinbeim JI, Couchman PR. *Macromolecules* 1983;16:589.
- [7] van der Sanden MCM, Meijier HEH, Lemstra PJ. *Polymer* 1993;34:2148.
- [8] Kinloch AJ, Young RJ. *Fracture behavior of polymers*. New York: Applied Sciences, 1983.
- [9] Eisenberg A. *Ions in polymers*, Adv. Chem. Ser. 187. Washington, DC: American Chemical Society, 1980.
- [10] Lundberg RD. In: Pineri M, Eisenberg A, editors. *Structure and properties of ionomers*. Dordrecht: Redel, 1987:429-438.
- [11] Agarwal PK, Makowski HS, Lundberg RD. *Macromolecules* 1980;13:1679.
- [12] Eisenberg A, Hird B, Moore RB. *Macromolecules* 1990;23:4098.
- [13] Bellinger M, Jar P, Sauer JA, Hara M. *ACS Polym Prepr* 1990;31(1):546.
- [14] Hara M, Bellinger M, Sauer JA. *Polym Int* 1991;26:137.
- [15] Weiss RA, Fitzgerald JJ, Kim D. *Macromolecules* 1991;24:1071.
- [16] Weiss RA, Agarwal PK, Lundberg RD. *J Appl Polym Sci* 1984;29:2719.
- [17] Smith P, Eisenberg A. *J Polym Sci, Polym Phys Ed* 1988;26:569.
- [18] Sullivan MJ, Weiss RA. *Polym Eng Sci* 1992;32:597.
- [19] Gao Z, Molnar A, Morin FG, Eisenberg A. *Macromolecules* 1992;25:6460.
- [20] Hong KM, Noolandi J. *Macromolecules* 1983;16:1083.
- [21] Bagrodia S, Wilkes HS, Kennedy JP. *Polym Eng Sci* 1986;26:662.
- [22] Huglin MB, Rego JM. *Polymer* 1990;31:1269.
- [23] Lee JY, Painter PC, Coleman MM. *Macromolecules* 1988;21:954.
- [24] de Ilarduya MA, Euiburu JL, Iruin JJ, Fernandez-Berridi MJ. *Makromol Chem* 1993;194:501.
- [25] de Mftahi MV, Frechet J. *Polymer* 1988;29:477.
- [26] Zhou Z-L, Eisenberg A. *J Polym Sci, Polym Phys Ed* 1983;21:595.
- [27] Weiss RA, Sen A, Willis CL, Pottick LA. *Polymer* 1991;32:1867.
- [28] Ihizu K, Kashi Y, Fukutomi T, Kakurai T. *Makromol Chem* 1982;183:3099.
- [29] Xu S, Huang B. *Preprints of First East Asian Symposium on Polymers for Advanced Technology*, The Chinese Academy of Sciences, 1997:48.
- [30] Pilz I, Kratky O. *J Colloid Interf Sci* 1967;24:11.
- [31] Rathje J, Ruland W. *Colloid Polym Sci* 1976;254:358.
- [32] Lake JA. *Acta Crystallogr* 1967;23:191.
- [33] Douglas E, Sakurai K, MacKnight WJ. *Macromolecules* 1991;24:6776.
- [34] Roe RJ. *Macromolecules* 1986;19:728.
- [35] Whitmore MD, Noolandi J. *Macromolecules* 1985;18:657.
- [36] Fox TG. *Bull Am Chem Soc* 1956;1:213.
- [37] Annighofer F, Gronski W. *Colloid Polym Sci* 1983;261:15.
- [38] Fitzgerald JJ, Weiss RA. *Columbic interaction in macromolecular system*. Washington, DC: American Chemical Society, 1986:35.
- [39] Colthup NB, Doly LH, Wiberly SE. *Introduction to infrared and raman spectroscopy*. New York: Academic Press, 1990.
- [40] Peiffer DG, Duvdevani I, Agarwal PK. *J Polym Sci, Polym Lett Ed* 1986;24:581.
- [41] Sakurai K, Douglas E, MacKnight WJ. *Macromolecules* 1993;26:209.
- [42] Yarusso DJ, Cooper SL. *Macromolecules* 1983;16:1871.
- [43] Register RA, Cooper SL. *Macromolecules* 1990;23:310.
- [44] Marx CL, Caulfield DF, Cooper SL. *Macromolecules* 1973;6:344.

- [45] MacKnight WJ, Taggart WP, Stein RS. *J Polym Sci, Polym Symp* 1974;45:113.
- [46] Roche EJ, Stein RS, Russell TP, MacKnight WJ. *J Polym Sci, Polym Phys Ed* 1980;18:1497.
- [47] Fitzgerald JJ, Weiss RA. *J Macromol Sci, Rev Macromol Chem Phys* 1988;C28:99.
- [48] Moore RB, Gauthier M, Williams CE, Eisenberg A. *Macromolecules* 1991;25:5769.
- [49] Guinier A, Fourné G. *Small-angle scattering of X-rays*. New York: Wiley, 1955.
- [50] Eisenberg A. *Macromolecules* 1970;3:147.
- [51] Helfand E, Sapse AM. *J Chem Phys* 1975;63:1327.
- [52] Noolandi J. *Polym Eng Sci* 1984;24:70.
- [53] Wu S. *Polym Eng Sci* 1987;27:335.